

REDUCTION OF IMPURITY SOURCES IN Si CRYSTAL GROWTH SYSTEM WITH ELECTRON GUN BEAM HEATING

A. Kravtsov ^a, J. Virbulis ^b, and A. Krauze ^b

^a KEPP EU, 5 Carnikavas Street, Riga, Latvia

^b Institute of Numerical Modeling, University of Latvia, 3 Jelgavas Street, Riga, Latvia

Email: doc@keppeu.lv

Received 18 December 2020; revised 19 May 2021; accepted 21 May 2021

A new series of experiments was conducted to determine the source of impurities in the process of silicon crystal growth with electron beam heating. A gas-dynamic window was placed between the electron gun and growth chamber. Also positively-charged traps were placed along the crucible to reduce the number of electrons hitting the chamber and the crucible. Five experiments were conducted: two with the window, two with charge traps, and one with both the window and charge traps.

The analysis of obtained samples showed that the gas-dynamic window decreases the content of Al, Cu, Fe, Cr and O₂, and the trap, used in the experiments, decreases the content of Fe, Cr and Cu in residues of the melt. The content of all impurities, except Al, is close to the goal level.

Al impurities come only from the gun, but the gas-dynamic window cannot eliminate them completely. It seems that Al impurities come either as neutral atoms carried by the gas or as positively charged ions. To reduce these impurities, a separation of the Al flow from the beam by the magnetic field is proposed.

Keywords: electron optics, materials testing and analysis, silicon, doping and ion implantation

PACS: 41.85.-p, 81.70.-q, 61.72.uf

1. Introduction

Growing single crystals by the Czochralski method has become widespread and is used in various ways, including growing pipes [1, 2], induction heating of the charge in a quartz crucible [3, 4], forced shaping (Stepanov's method) [5] and growing crystals with a low temperature gradient [6]. The most widespread is the method of growing single crystals from a crucible with resistive heating, which is used for growing silicon single crystals. In all of these methods, the melt comes into contact with the crucible, which is a source of contamination. A number of attempts have been made to organize the process without contact of the silicon melt with the container – in the skull, using electron beam heating [7, 8]. These processes have not found a wide application since they faced the difficulty of increasing the diameter of the growing crystal more than 40 mm. Our article is

devoted to the results obtained during the development of the process of growing silicon crystals from a skull using electron beam heating [9], in which growing crystals with a diameter of 150–200 mm is common. In this process, using a quartz crucible (not a skull), we obtained a rod with a diameter of 300 mm and a mass of 80 kg. Some research results were published earlier [10, 11]. Silicon is heated by two cold-cathode electron-beam heaters (EBH) that use a gas mixture of hydrogen and less than 1% oxygen. The process is carried out using a cold crucible, which is insulated from silicon by a heat insulator [9]. On the one side, it was shown that the purity of the rod for most of the controlled impurities is comparable to the purity of the reference sample – silicon obtained in the float-zone (FZ) process by the first-class producer. On the other side, the whole spectrum of metallic impurities was observed in the silicon residues after the process, indicating

the introduction of contaminants into the melt during the growth process. The spectrum of the main impurities in the remnants of the melt and the alleged sources of their formation are shown [9] in Fig. 1. Based on the achieved sensitivity of the methods for determining the impurity concentration, it is advisable to control their content not in the grown crystal, where, due to the smallness of the distribution coefficients of metallic impurities, their content is not significant, but in the remainder of silicon from the process, enriched by the introduced impurities [9]. In order to establish the sources of introduced pollution and to find ways of reducing it, the experimental work described below was carried out.

Under the influence of the applied voltage, in the gas-discharge chamber of an electron beam heater with a cold cathode, plasma ions bombard the cathode and initiate the creation of electrons directed to the treated surface, in our case, to silicon [12]. Part of the high-energy particles bombard all surfaces of the gas-discharge chamber and the beam guide. In these collisions, metal atoms are knocked out of all the contacted surfaces, both in the form of neutral atoms and ions. Together with the gas and the electron beam, they enter the process chamber and the surface to be treated. Based on the results of [9], we assume that it is necessary to eliminate the gas flow from the EBH to remove the mentioned impurities. In addition, electrons entering the process chamber and reflecting from the treated surface can contact the ma-

terials of the container and the process chamber. We consider that it is necessary to try to eliminate such a contact. In the case of metallurgical processing of metals, these processes can be neglected, but for pure materials of semiconductor applications the concentration of these impurities can be important.

To estimate the dispersion of electrons in the beam on the basis of the model [12], we measured the distribution of electrons near the surface of the melt located at 500 mm (experimental processes, Fig. 2) and 1200 mm (the process described in [9], the data of which are shown in Fig. 1).

2. Experiments and data

The general scheme and photographs of the organization of experimental processes are shown in Fig. 2.

In the experiments, the design of the cold crucible was partially changed and was made only of copper, the heat insulator and other structural materials were excluded. Above the copper crucible, in the direction where, according to the optical laws, the electron beam reflected from the melt should have entered, a plate was installed, to which a potential of +70 V was applied, in order to influence the intensity of the bombardment of the technological chamber surface by reflected electrons. This plate was called the ‘trap’. In the experiments, the power developed by EBH

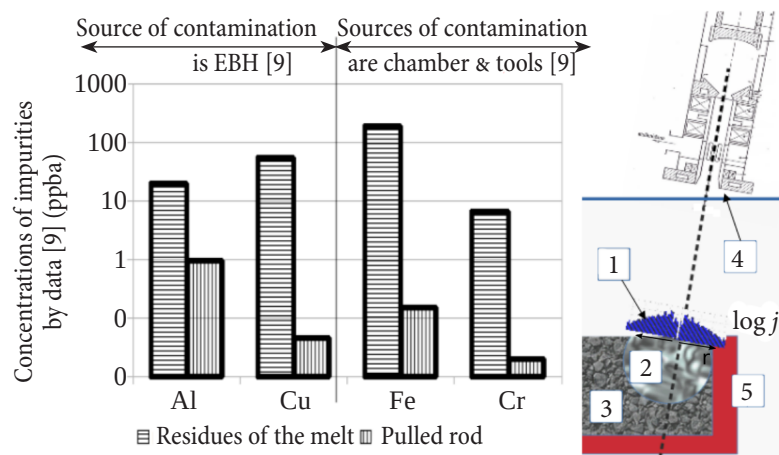


Fig. 1. Contaminations of residue of the melt in the process of pulling of silicon crystals with electron beam heating [9] and the beam position with the calculated electron distribution in such process. 1, electrons distribution; 2, melt; 3, raw silicon rocks; 4, electron beam heater (EBH); 5, heat insulation.

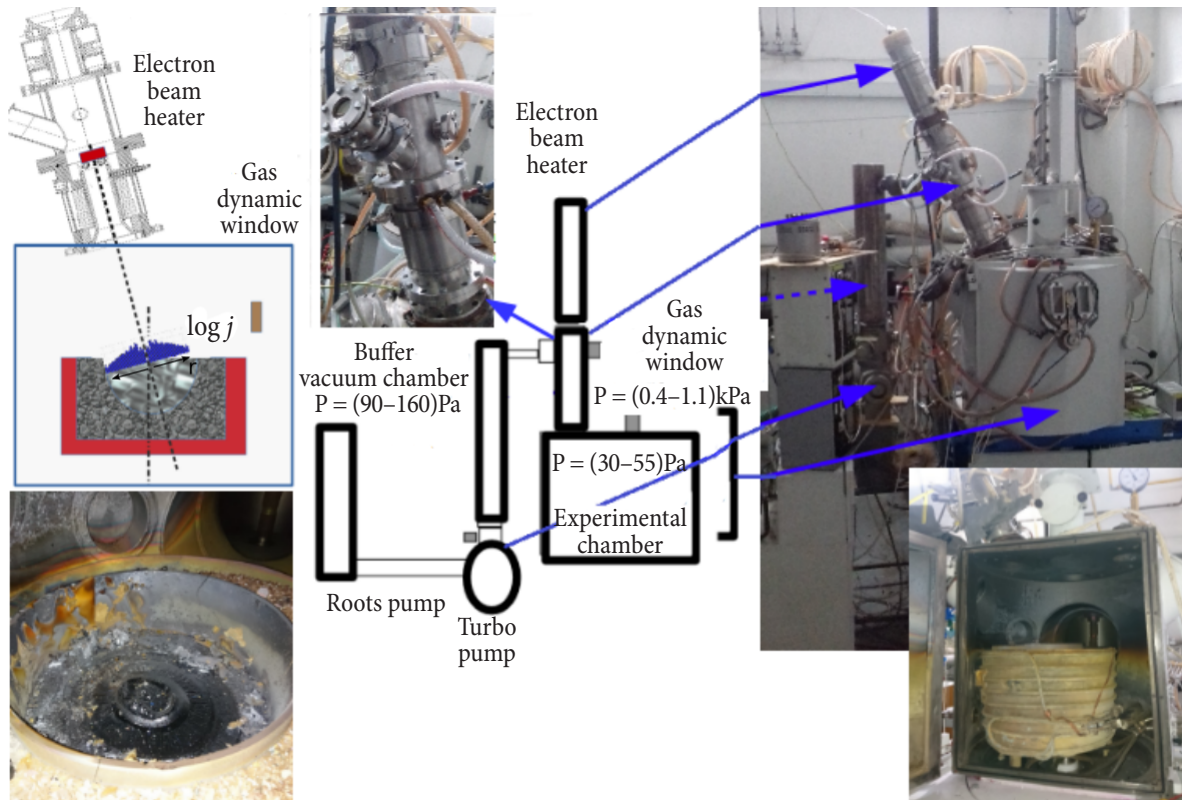


Fig. 2. Experimental setup. The electron beam heater, gas-dynamic window and calculated distribution of electrons on Si (left above), the rest melt after the crystal growth experiment (left below), a schematics of the growth system (middle), a picture of the growth system (right above), the growth chamber with a cold crucible (right below).

was close to power that was used in the growing process described in [9]. The distribution of electrons near the surface of the melt in scale is plotted on the axis of the beam that heated the melt. In each experiment, the melt was kept for 6 h at a given power to saturate with impurities, and gradually crystallized. Samples for control were taken as close as possible to the last crystallized melt drop.

A gas-dynamic window (GDW) equipped with a membrane was installed between the EBH and the process chamber. Argon was brought to the membrane from below, and an additional evacuation system was installed above the membrane using a turbomolecular pump. Before starting the processes, the gas-vacuum system of the installation was adjusted in order to supply argon in an amount sufficient to significantly reduce the flow rate of plasma-forming gas, while maintaining the same residual pressure in the process chamber. As a result, the residual pressure in the process chamber was maintained in a range of 30–55 Pa, in the pumped-out part of the GDW it was 400–1100 Pa, and in the buffer chamber, near the turbomolecular pump,

the pressure was 90–160 Pa when a power of about 40 kW was released in the heater that corresponds to the power of one heater during the growing process described in [9].

The area of silicon melting was located near the centre of the quartz crucible. The serial numbers of the processes carried out on the experimental installation VU 1 are 80–85. In processes 80 and 81, only GDW was used, in processes 82–83 only ‘traps’, and in process 85 ‘traps’ and GDW were used. The first attempt in the process with the combined use of GDW and traps (process 84) failed due to a poor beam control. From each process (80–83 and 85) 3 samples were taken, the content of impurities in which was controlled by the ICP MS method¹, and 1 sample for monitoring the oxygen content by FTIR spectroscopy² at room temperature.

¹ The authors are grateful to Dr. Sylke Meyer (Fraunhofer Center for Silicon photovoltaics) for measurements and an interesting discussion of the results.

² The authors are grateful to Dr. Georgy Chikvaidze (Institute of Solid State Physics of Latvian University) for the measurements and interesting discussion of the results.

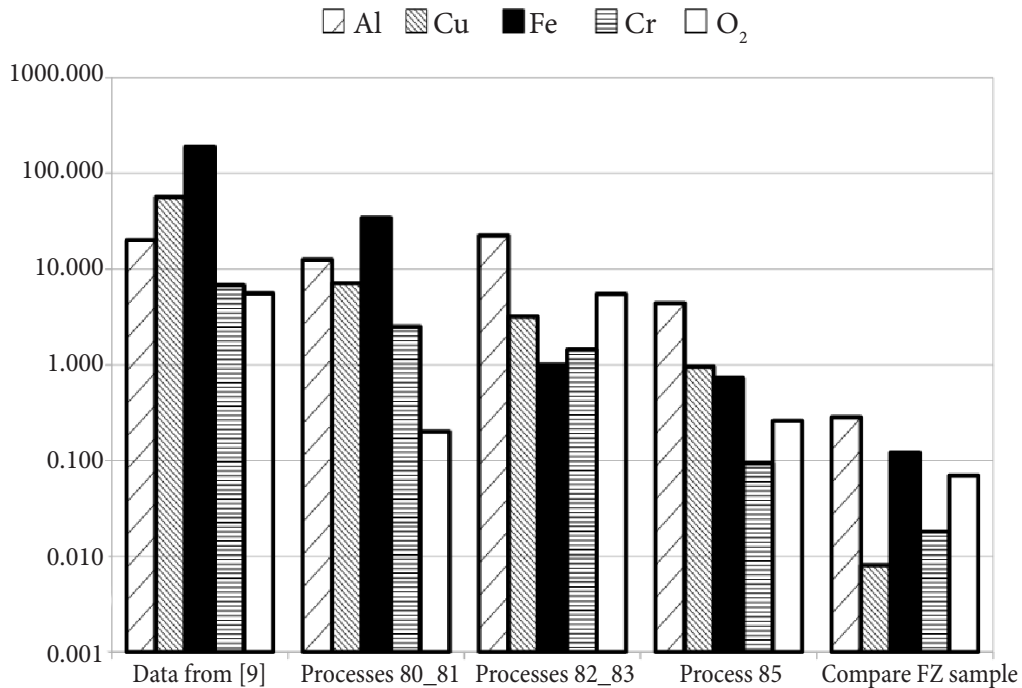


Fig. 3. Content of impurities in the remains of the melt after the growth process with electron beam heating and with/without GDW and 'trap'. (a) Metals in ppba, (b) oxygen in ppma.

Based on the average values of the content of impurities for 3 samples in each process, histograms of changes in the concentrations of all impurities, with a concentration of more than 1 ppba, are shown in Fig. 3. The results of the control of undoped monocrystalline FZ silicon, designated as NHR, cut from a sample of serial production with a specific electrical resistance of more than 3000 Ω -cm of N type of electrical conductivity are also shown here. The presence of metallic impurities in this sample can be taken as the level of error in control measurements, since verification of the same sample for aluminium content by LT FTIR spectroscopy showed that the aluminium concentration in it was below the detection limit (ppba units). The oxygen concentration in the samples from the process described in [9] is shown in Fig. 1 and processes 80–83 and 85 determined by FTIR at room temperature are shown in Fig. 3. The comparison between the impurity concentrations in Figs 1 and 3 showed that the introduction of GDW lead to a decrease in the concentration of oxygen, copper, iron, chromium and aluminium. Concentrations of these impurities decreased significantly: iron from 190 to 34 ppba, copper from 60 to 8 ppba, chromium from 7 to 2.5 ppba and aluminium from 20 to 12 ppba, and the oxygen content in silicon

decreased from 5 to 0.2 ppma. The concentration of all impurities, except for aluminium and oxygen, decreased when the 'traps' were turned on. The concentration of iron and chromium decreased to a level commensurate with the NHR sample, and copper fell to 3.5 ppba. The concentration of impurities of alkali metals Na and Ca and concentrations of antimony are not exceeding 1 ppba, in comparison with the results of the growing process described in [9].

3. Discussion of experimental results

Impurities have not been found in the experimental processes, but were presented in the process described in [9]. Impurities of Na, Ca and Sb in the experiments are absent, and most likely it indicates the absence of their sources in the processes performed. The source of antimony was the silicon dust from the inner surface of the chamber specially deposited on this surface in the course of the processes carried out before the process described in [9] by processing silicon doped with antimony. The source of sodium and potassium could be a heat insulator used in the growing process [9] and not used in laboratory processes. The calculations of the distribution area of electrons around the electron beam trajectory

in the case when the EBH is situated 1200 mm above the melt shown in Fig. 1 and contacts of the part of electrons with heat insulations are obvious.

Carrying out processes with GDW without ‘traps’ showed that concentrations of all impurities were changed. The concentrations of aluminium with the use of GDW decreased by 2 times, that of chromium by 3 times, the concentration of copper and iron dropped by 5 times, and that of oxygen by 25 times. Hence, it follows that atoms of all these impurities entered the melt from the EBH by gas transport (Fig. 3).

When carrying out processes with a ‘trap’ (processes 82 and 83), the level of impurities decreased: iron from 190 to 1 ppba (by 190 times), chromium from 7 to 1.5 ppba (5 times) and copper concentration decreased from 57 to ~3.2 ppba (18 times). Concentrations of aluminium and oxygen were not changed. The copper, iron and chromium concentration in the 85 process (with GDW and the ‘trap’) decreased to approximately 1 ppba or less, and came to the level as in the NHR sample.

The GDW unequivocally decreased the concentration of aluminium in the process, but a quantity assessment of the influence of GDW on the aluminium concentration is difficult. The level of aluminium determined by the ICP MS method in the NHR sample, where it was virtually absent, was 6 ppba. The aluminium concentration in the process with GDW and with GDW and a ‘trap’ changed from 12 to 4.5 ppba. If we consider the result of measuring the concentration of aluminium in NHR as a measurement error, then it is difficult to make an unambiguous conclusion about the positive effect of

the ‘trap’ on the decrease in the amount of aluminium in silicon. The oxygen concentration in the processes with the ‘trap’ did not change, and with the GDW and the ‘trap’ did not differ from the processes only with the GDW.

Thus, it can be stated that GDW reduces the chromium, copper and iron concentrations, slightly reduces the aluminium concentration, and radically decreases the oxygen concentration in the melt residues after the process. This is ensured by the supply of pure argon to the GDW, which ‘blocks’ the flow of the hydrogen–oxygen mixture from the EBH in the volume of GDW, from where the hydrogen–oxygen mixture together with argon is forcibly removed by an additional vacuum pump.

Studying the nature of the impact of the ‘trap’ we should state the following. High-energy electrons penetrate to a considerable depth in the treatment object, for example, such electrons, having passed through a metal several centimetres thick, practically did not change their energy, while a hole in the metal did not appear [13]. In our experiments with a system as described in [9], but with a non-moving electron beam, we observed a similar effect – the deformation of a quartz crucible on the axis of the beam passing through a layer of molten silicon with a thickness of more than 100 mm. All the high-energy electrons came in the melt (excluding the reflected part of these electrons). Evaluating the results obtained on reducing the contamination of the melt with iron, chromium and copper, we assumed that a significant number of electrons with lower energy are possibly formed, which interact with the chamber walls and the copper crucible. To test the feasibility

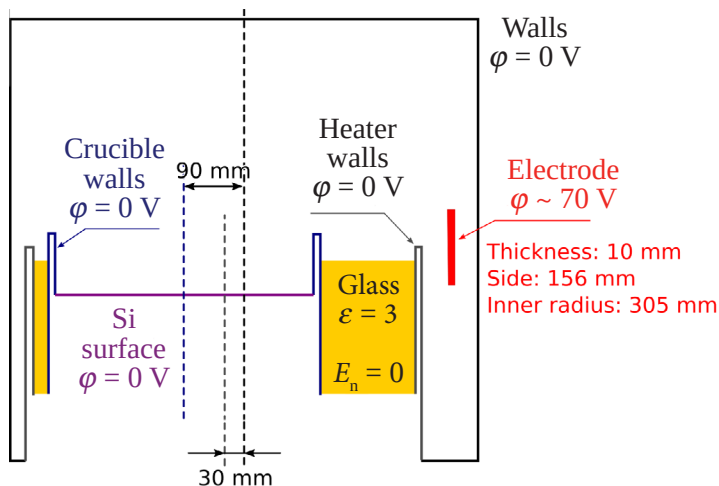


Fig. 4. The scheme and conditions accepted in the calculations.

- Electrostatic problem
 - $\Delta\varphi = 0$, except electrode
 - Second order finite elements, gmsh
- Chamber, crucible, heater walls are grounded
- Electrode potential ~70 V
 - Modelled via sources
- Electron trajectory equation:

$$\frac{d}{dt} \frac{m\vec{v}}{\sqrt{1 - \frac{v^2}{c^2}}} = q\vec{E}$$

of this assumption, calculations were performed to assess the effect of the electric field of the trap on electrons. The design scheme and the used conditions are shown in Fig. 4.

As a result of the calculations for electrons with low energy and doubly reflected electrons, we obtained the data presented in Fig. 5.

From the presented data, it follows that the electric field of the electrode cannot act on electrons with energies of 30 eV, the effect on electrons with energies of 3.0 eV is extremely small, and the threshold energy for knocking out an iron atom is 4.3 eV. Thus, the electrode can act on the primary reflected electrons with an energy of less than 3.0 eV and

on electrons with an energy of 0.3 eV, that are secondarily reflected from the camera. The energy of those electrons that can be affected by the created electric field is not enough to knock out the iron atoms. Hence the assumption that these electrons cannot be the cause of the contamination of residues in the melt with iron and chromium and cannot be the second source of contamination with copper. We will continue to investigate the nature of the observed phenomenon.

The source of silicon contamination with aluminium is only EBH, since there were no other aluminum parts in the experimental chamber. The use of GDW does not completely eliminate

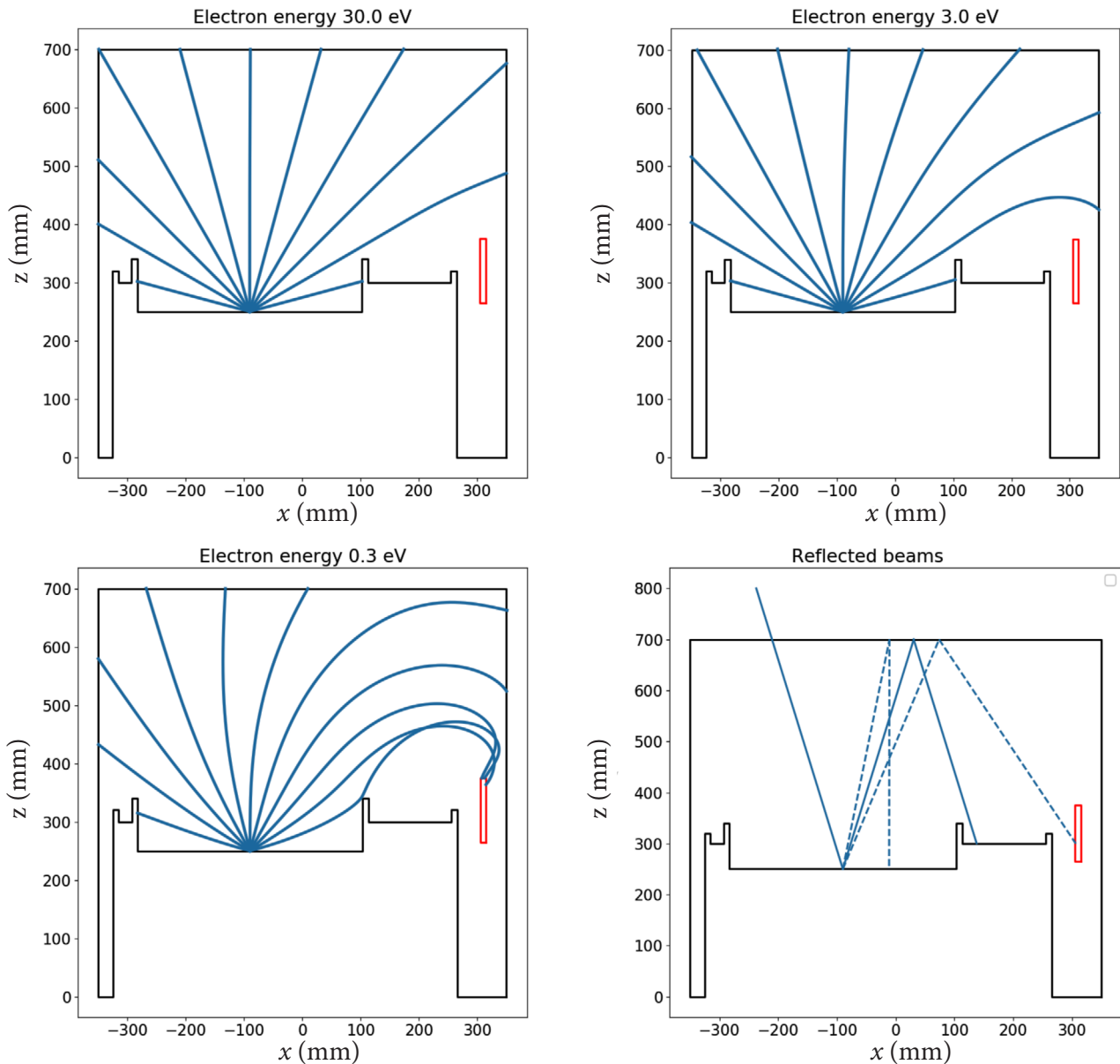


Fig. 5. Interaction of low energy electrons with the electrode used in the experiments.

the resulting pollution. Theoretically atoms knocked out of EBH materials can be in two states: electrically neutral atoms transported by the gas flow and positive ions framing the electron beam. Apparently, aluminum is present in both forms and the removal of its atoms from the gas stream does not provide the required process purity. In our opinion, magnetic separation is most applicable here.

4. Conclusions

The application of a GDW substantially reduced the contamination of silicon melt with chromium, iron, copper, aluminium and oxygen. The use of a positive electrode ('trap') reduced the contamination of silicon melt with iron, chromium and copper, that are presumably introduced by the irradiation of structural elements inside the technological chamber. The combination of GDW and a positive electrode ('trap') allowed us to reach the concentration level within 1–5 ppba for all mentioned impurities in the melt residues. Consequently, the concentration of metallic impurities with low distribution coefficients in the grown Si crystal (copper 10^{-4} , chromium 10^{-5} , iron 10^{-6}) will be less than 0.1 ppta. The estimated aluminium concentration (distribution coefficient) in the rod will be around 200 ppta, which is permissible for the production of silicon with a resistance of less than 50 $\Omega\cdot\text{cm}$ without long-term high-temperature heat treatment.

Acknowledgements

The research leading to these results has been supported by the European Regional Development Fund Project 'Competence Centre of Mechanical Engineering', Contract ID No. 1.2.1.1/18/A/008 signed between the Competence Centre of Mechanical Engineering and the Central Finance and Contracting Agency, Research No. 2.1 'Process Research and Optimized Development of Electron Beam Heater for Production of High Purity Materials'.

References

- [1] K. Lebovic, *Monocrystalline Tubular Semiconductor*, US Patent 2890976 (1959).
- [2] V. Bevez, L. Berezenko, S. Gashenko, N. Danilevko, Y. Jepikhin, Y. Timoshin, and E. Falkevich, *Method of Producing Hollow Silicon Tubes*, USSR Author's Certificate SU 687654 (1987).
- [3] O.I. Podkopaev and A.F. Shimanskiy, *Growth of Germanium Single Crystals with a Low Content of Dislocations and Impurities*, monograph (Siberian Federal University, Krasnoyarsk, 2013) [in Russian].
- [4] H. Riemann, N.V. Abrosimov, J. Fischer, B.M. Renner, and K. Wusterhausen, *Method and Apparatus for Producing Single Crystals Composed of Semiconductor Material*, US Patent Application Publication No. US 2012/0285369 A1 (2010).
- [5] P.I. Antonov et al., *Obtaining Profiled Crystals and Products by the Stepanov Method* (Nauka, Leningrad, 1981) [in Russian].
- [6] Ya.V. Vasilev, Yu.A. Borovlev, E.N. Galashov, N.V. Ivannikova, F.A. Kuznecov, A.A. Pavlyuk, Yu.G. Stenin, and V.N. Shlegel', Low-gradient technology for growing the scintillating oxide crystals, in: *Scintillation Materials*, collection (Kharkov, 2011) pp. 119–180, http://www.niic.nsc.ru/attachments/article/2327/LTG_review.pdf [in Russian].
- [7] Ch.W. Hanks and Ch.d'A. Hunt, *Method for Growing Crystals*, US Patent 3494804, A Continuation-in-part of application Ser. No. 659, 175, Aug. 8 (1967).
- [8] T.F. Ciszek, Growth of 40 mm diameter single crystals by a pedestal technique using electron beam heating, *J. Cryst. Growth* **12**, 281–287 (1972).
- [9] An. Kravtsov, Developing of silicon growth techniques from melt with surface heating, *IOP Conf. Ser. Mater. Sci. Eng.* **355**, 012037 (2018).
- [10] An. Kravtsov, Novel metod for feedstock production for high efficiency FZ c-Si PV, *IOP Conf. Ser. Mater. Sci. Eng.* **77**, 012007 (2015).
- [11] An. Kravtsov, Al. Kravtsov, R. Fuksis, and M. Pudzs, Ingot pulling with electron beam heating: process enhancements, in: *Proceedings of 2015 IEEE 42nd Photovoltaic Specialist Conference (PVSC)* (New Orleans, LA, 2015) pp. 1–4.
- [12] A. Krauze, J. Virbulis, and An. Kravtsov, Modeling electron beam parameters and plasma interface

position in an anode plasma electron gun with hydrogen atmosphere, IOP Conf. Ser. Mater. Sci. Eng. 355, 012008 (2018).

[13] I.S. Hasanov, *Plasma and Beam Technology* (Elm, Institute of Physics, National Academy of Sciences of the Azerbaijan Republic, 2007).

PRIEMAIŠŲ ŠALTINIŲ MAŽINIMAS SI KRISTALŲ AUGINIMO SISTEMOJE SU KAITINANČIU ELEKTRONŲ PATRANKOS PLUOŠTU

A. Kravtsov^a, J. Virbulis^b, A. Krauze^b

^a KEPP EU, Ryga, Latvija

^b Latvijas universiteto Skaitmeninio modeliavimo institūtas, Ryga, Latvija